

The LPM effect in sequential bremsstrahlung: from large- N QCD to $N=3$ via the $SU(N)$ analog of Wigner 6- j symbols

Peter Arnold

*Department of Physics, University of Virginia,
Charlottesville, Virginia 22904-4714, USA*

(Dated: December 15, 2024)

Abstract

Consider a high-energy parton showering as it traverses a QCD medium such as a quark-gluon plasma. Interference effects between successive splittings in the shower are potentially very important but have so far been calculated (even in idealized theoretical situations) only in soft emission or large- N_c limits, where N_c is the number of quark colors. In this paper, we show how one may remove the assumption of large N_c and so begin investigation of $N_c=3$ without soft-emission approximations. Treating finite N_c requires (i) classifying different ways that four gluons can form a color singlet and (ii) calculating medium-induced transitions between those singlets, for which we find application of results for the generalization of Wigner 6- j symbols from angular momentum to $SU(N_c)$. Throughout, we make use of the multiple scattering (\hat{q}) approximation for high-energy partons crossing quark-gluon plasmas, and we find that this approximation is self-consistent only if the transverse-momentum diffusion parameter \hat{q} for different color representations satisfies Casimir scaling (even for strongly-coupled, and not just weakly-coupled, quark-gluon plasmas). We also find that results for $N_c=3$ depend, mathematically, on being able to calculate the propagator for a coupled non-relativistic quantum harmonic oscillator problem in which the spring constants are operators acting on a 5-dimensional Hilbert space of internal color states. Those spring constants are represented by constant 5×5 matrices, which we explicitly construct. We are unaware of any closed form solution for this type of harmonic oscillator problem, and we discuss prospects for using numerical evaluation.

I. INTRODUCTION

Very high energy particles traveling through a medium lose energy primarily through splitting via bremsstrahlung and pair production. At very high energy, the quantum mechanical duration of each splitting process, known as the formation time, exceeds the mean free time for collisions with the medium, leading to a significant reduction in the splitting rate known as the Landau-Pomeranchuk-Migdal (LPM) effect [1, 2]. In the case of QCD, the basic methods for incorporating the LPM effect into calculations of splitting rates were developed in the 1990s by Baier et al. [3, 4] and Zakharov [5] (BDMPS-Z). More recently, there has been interest in how to compute important corrections that arise when two consecutive splittings have overlapping formation times.¹ As we'll discuss, such calculations must generically address a non-trivial problem of how to account for the color dynamics of the high-energy partons as they split while interacting with the medium. This problem has been sidestepped in overlapping formation time calculations to date by taking either (i) the soft bremsstrahlung limit [6–8] or (ii) the large- N_c limit [9–12]. In this paper, we show how to avoid these limits by showing how to incorporate the full color dynamics. But readers need not appreciate the full history and formalism of the subject to follow most of this paper: the problem we most need to address will be an application of $SU(N)$ group theory to (i) the different ways to make color singlets from four partons and (ii) transitions between those singlets due to interactions with the medium. The latter will involve the $SU(N)$ generalization of Wigner 6- j coefficients. The original purpose of Wigner 6- j coefficients can be thought of as describing for angular momentum [symmetry group $SU(2)$] the relation of different bases for spin singlet states made from four spins.² In our case, we will need the generalization from spin to color.

The relevance of studying 4-particle color singlets can be qualitatively understood by adapting, to the discussion of (overlapping) sequential splitting, a picture originally used by Zakharov [5] to discuss single splitting. Consider an initial high-energy parton (quark or gluon) with energy E that splits twice in the medium to make three high-energy daughters, with energies xE , yE and $(1-x-y)E$. Fig. 1a shows an example of a contribution to the total rate from an interference between one way the splitting can happen in the amplitude and another way it can happen in the conjugate amplitude. The diagrams are time-ordered from left to right (and the vertex times should be integrated over). Fig. 1b shows an alternative way of depicting this contribution by sewing the amplitude and conjugate amplitude diagrams together into a single diagram for this particular interference contribution to the rate. Adapting Zakharov's picture, we can recast the calculation by *formally* re-interpreting the right-hand diagram as instead representing (i) three particles propagating forward in time, followed by a splitting into (ii) four particles propagating forward in time [shaded region], followed by a recombination into (iii) three particle propagating forward in time.³ Only the high-energy particles are explicitly drawn in fig. 1: each is interacting many times with the

¹ For one summary of why this is an interesting problem, see, for example, the introduction of ref. [14].

² In textbooks, Wigner 6- j coefficients are often described instead as related to the coupling of three different angular momenta j_1 , j_2 , and j_3 to make a fourth J . (See, for example, section 6.1 of ref. [15].) But since J can be combined with a fourth angular momentum j_4 to make a singlet if and only if $J = j_4$, this is the same problem as how to combine four angular momenta j_1 , j_2 , j_3 and j_4 to make a singlet.

³ There is a technical assumption here that one has integrated the rate over the transverse momenta of the final daughters. See section IV.A of ref. [9] and appendix F of ref. [10] for more details.

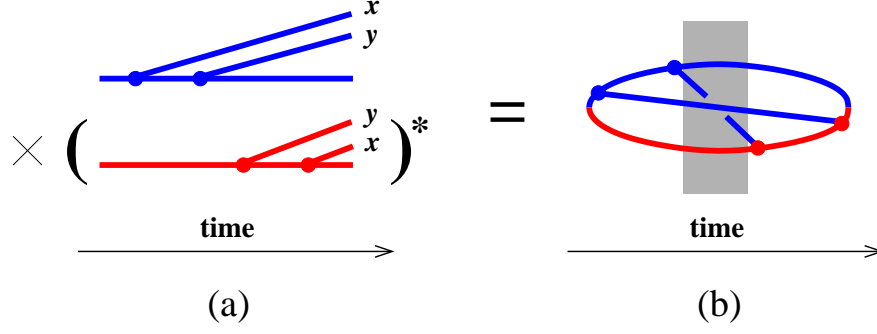


FIG. 1: An example of an interference contribution to the rate for (overlapping) sequential splitting, with blue indicating the amplitude and red the conjugate amplitude. In (b), the shading highlights the region of time where the evolution must track *four* high-energy particles (three in the amplitude and one in the conjugate amplitude).

medium, and a statistical average over the medium is performed to get the (average) rate. In actual calculations, the evolution of the system during the three stages (i), (ii), and (iii) just described can be treated as an effective Schrödinger-like problem for the evolution of the transverse positions of the high-energy particles. The drawing of fig. 1b suggests, by color conservation (after medium averaging), that the high-energy particles should form an overall color singlet during each stage of evolution. Because there are multiple ways for four color charges to form a color singlet, the color dynamics of the shaded region of fig. 1b can be non-trivial.

In more detail, ref. [16] discusses how the potential energy for the Schrödinger-like evolution equation can be defined in terms of multi-particle Wilson loops involving lightlike Wilson lines. These are generalizations of the 2-particle Wilson loops that were introduced by Liu, Rajagopal, and Wiedemann [17, 18] as a way to define the medium parameters \hat{q}_R for strongly-interacting plasmas. Physically, \hat{q}_R characterizes the momentum-space diffusion relation $\langle Q_\perp^2 \rangle = \hat{q}_R \Delta z$ for the net transverse momentum kick \mathbf{Q}_\perp a high-energy particle picks up from traversing distance Δz through the medium, for sufficiently large Δz . Here, \hat{q}_R depends on the color representation R of the high-energy particle (e.g. fundamental representation for quarks and adjoint representation for gluons). In this paper, we start from the result of ref. [16] that the multi-particle potentials that are needed for the calculations represented by fig. 1b are harmonic oscillator potentials that can be written in terms of \hat{q} as

$$\underline{V}(\mathbf{b}_1, \mathbf{b}_2, \dots, \mathbf{b}_n) = -\frac{i}{8} \sum_{i>j} (\hat{q}_i + \hat{q}_j - \underline{\hat{q}}_{ij}) (\mathbf{b}_i - \mathbf{b}_j)^2 \quad (1.1)$$

in the high energy limit, for which the transverse separations of the particles are small. (This high-energy approximation has the same technical caveats, reviewed in ref. [16], as most all other applications of \hat{q} .) Above, the \mathbf{b}_i are the transverse positions of the high-energy particles during any particular stage of the evolution. \hat{q}_i represents the value of \hat{q} for the i -th particle. $\underline{\hat{q}}_{ij}$ represents the value of \hat{q} for the color representation corresponding to the *combined* color representation of particles i and j . In the general case, this combined color representation is not unique. For example, if the i and j represent gluons (which are each in the 8-dimensional adjoint representation of color), then the combination of the two could be any irreducible representation in the SU(3) tensor product $\mathbf{8} \otimes \mathbf{8} = \mathbf{1} \oplus \mathbf{8} \oplus \mathbf{8} \oplus \mathbf{10} \oplus \overline{\mathbf{10}} \oplus \mathbf{27}$.

Since the values of \hat{q} are mostly different for each irreducible representation, the \hat{q}_{ij} in (1.1) is not a single number but instead an operator (which can be represented by a finite-dimensional matrix) acting on the color space of the N particles. Following ref. [16], we use underlining to indicate which quantities are color operators in (1.1).

Ref. [16] discusses why the color structure of the n -particle potential (1.1) is trivial for $n=3$ because overall color conservation then implies $\underline{\hat{q}}_{12} = \hat{q}_3$ and permutations. But the color structure is *not* trivial for $n=4$, which is needed for evolution of the shaded part of fig. 1b.

One main goal of this paper is to find the explicit matrix formula for (1.1) for the case of four gluons, relevant to the calculation of overlap effects for double bremsstrahlung $g \rightarrow ggg$. We will review how there are eight ways to make a color singlet from four gluons. But we will give a symmetry argument that three of those singlets decouple from the color dynamics of $g \rightarrow ggg$, leaving us with a 5-dimensional subspace of 4-gluon color singlet states, which mix dynamically due to interactions with the medium. Correspondingly, we will show how $\underline{V}(\mathbf{b}_1, \mathbf{b}_2, \mathbf{b}_3, \mathbf{b}_4)$ is explicitly implemented by a 5×5 matrix function that is quadratic in transverse separations. We'll also perform the analysis for $SU(N_c)$ with $N_c > 3$, to see how potentials previously used in large- N_c calculations of overlap effects are recovered as $N_c \rightarrow \infty$.

With explicit results for the 4-gluon potential in hand, we demonstrate that consistency of the \hat{q} approximation for this application necessarily implies that \hat{q} satisfy Casimir scaling (i.e. $\hat{q}_R \propto C_R$, where C_R is the quadratic Casimir of color representation R) for the specific representations relevant to this paper (those generated by $\mathbf{8} \otimes \mathbf{8}$). We suspect that Casimir scaling is necessary more generally, but so far we have not pursued a more general argument. Though Casimir scaling of \hat{q} has long been known through next-to-leading order for weakly-coupled plasmas [19], we are unaware of a previous argument for Casimir scaling in applications to finite- N_c strongly-coupled plasmas (again subject to the technical caveats of the \hat{q} approximation reviewed in ref. [16]).

The last goal of this paper is to discuss how to use the explicit potential to calculate overlap effects for $g \rightarrow ggg$ in $N_c=3$ QCD. Though we will write formulas that can in principle be implemented numerically, the practical problem of implementing those numerics will be much more complicated than the case of large- N_c QCD, and we do not attempt it today. We will see that the problem involves finding the propagator for a quantum system of two coupled harmonic oscillators whose spring constants are finite-dimensional matrices in a space of additional quantum degrees of freedom:

$$\underline{H} = \frac{p_1^2}{2m_1} + \frac{p_2^2}{2m_2} + \frac{1}{2} \begin{pmatrix} q_1 \\ q_2 \end{pmatrix}^\top \begin{pmatrix} \underline{a} & \underline{b} \\ \underline{b} & \underline{c} \end{pmatrix} \begin{pmatrix} q_1 \\ q_2 \end{pmatrix}, \quad (1.2)$$

where here \underline{a} , \underline{b} , and \underline{c} are constant (5×5) symmetric matrices that do not all commute, q_1 and q_2 are two position degrees of freedom, p_1 and p_2 are the corresponding conjugate momenta, and the “masses” m_1 and m_2 are constants (unrelated to actual particle masses, which we ignore). As we'll discuss, the matrix structure of the spring constants makes computing and using the propagator for the system (1.2) more difficult for $N_c=3$ than for the large- N_c limit.

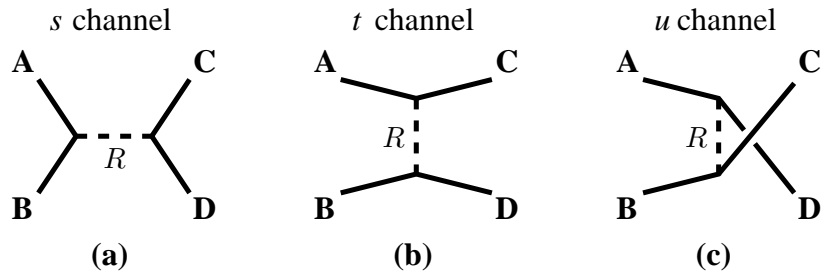


FIG. 2: Different ways of making a basis of singlet states for four particles.

Outline

In the next section, we first discuss the different ways that four gluons can make an $SU(3)$ color singlet, and the transformations between different basis choices needed to determine the \hat{q}_{ij} in (1.1) in terms of the values \hat{q}_R for different color representations. Explicit transformations may be found in terms of 6- j coefficients taken from the literature [20]. We also discuss the permutation symmetries that reduce the 8-dimensional space of singlets to the 5-dimensional subspace relevant for our application.

In section III, we find the 4-body potential in the harmonic approximation (1.1) by explicitly constructing the matrices \hat{q}_{ij} . We show that consistency of the color structure of that potential requires that \hat{q}_R satisfy Casimir scaling.

In section IV, we briefly review that, for this application, ref. [9] showed how to use symmetry to reduce the 4-body evolution problem to an effective 2-body evolution problem, and we explicitly construct the corresponding harmonic oscillator Hamiltonian. In each of the two transverse dimensions, we will see that the problem has the form (1.2).

Section V discusses the generalization of our analysis to $SU(N_c)$ for $N_c > 3$, which has an interesting twist requiring discussion of how it smoothly matches to $N_c = 3$. We use the $SU(N_c)$ results to see exactly how the color dynamics found in this paper approaches the simpler large- N_c results used in previous work on overlapping formation times.

Section VI gives our conclusion, where we discuss the difficulty of matrix-coefficient harmonic oscillator problems like (1.2) and the prospect for numerics.

In the appendix, we outline our own calculation of $SU(N_c)$ 6- j coefficients involving four gluons. We carried this out in part because the list of coefficients we need is not quite complete (for $N_c > 3$) in the previous literature, and in part to independently confirm previous calculations.

II. COLOR SINGLETS AND 6- j COEFFICIENTS FOR 4 GLUONS

A. Basics

One way to make a basis of color singlet states from 4 particles (which here we'll call A, B, C, and D) is depicted in fig. 2a. Consider an irreducible color representation R that appears in both (i) the tensor product $R_A \otimes R_B$ of the color representations of particles A and B and (ii) the tensor product $R_C \otimes R_D$ of particles C and D. Combine AB to make R and combine CD to make R , and then combine those two R 's to make a singlet.

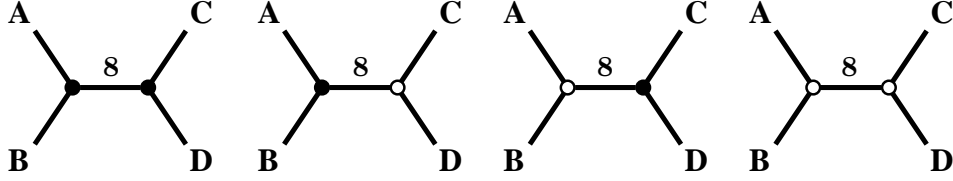


FIG. 3: Different ways to make the $R=8$ case of fig. 2a. Closed and open circles represent the anti-symmetric and symmetric combinations $\mathbf{8}_a$ and $\mathbf{8}_s$, respectively.

There is nothing special about choosing to first make the combinations AB and CD. We could have just as well chosen AC and BD, or AD and BC. We'll refer to these as s -channel, t -channel, or u -channel choices of bases for the color singlet states, as depicted in figs. 2(a–c) respectively.

The relevant tensor product for combining two gluons is

$$\mathbf{8} \otimes \mathbf{8} = \mathbf{1}_s \oplus \mathbf{8}_a \oplus \mathbf{8}_s \oplus \mathbf{10}_a \oplus \overline{\mathbf{10}}_a \oplus \mathbf{27}_s, \quad (2.1)$$

where the subscripts give the additional information of whether each irreducible representation arises in the symmetric (s) or anti-symmetric (a) combination of $\mathbf{8} \otimes \mathbf{8}$. The decomposition (2.1) means that there are five possibilities ($\mathbf{1}$, $\mathbf{8}$, $\mathbf{10}$, $\overline{\mathbf{10}}$, and $\mathbf{27}$) for the R of fig. 2a to obtain color singlets from four gluons. However, there are more than five singlet possibilities because there are two different ways ($\mathbf{8}_a$ and $\mathbf{8}_s$) each pair of gluons (AB or CD) can make an $\mathbf{8}$, and so there are four different color singlets corresponding to the case $R=8$ in fig. 2a. Following the notation of ref. [20], one could denote these four singlets by fig. 3, where a closed circle at a vertex indicates the anti-symmetric combination $\mathbf{8}_a$ of (2.1) and an open circle represents the symmetric combination $\mathbf{8}_s$. Because of this multiplicity, there are in total eight independent color singlets that can be made from four gluons. The different channels of fig. 2 just provide different ways to choose a basis for the eight-dimensional space of 4-gluon singlets. In what follows, we'll refer to the s -channel basis of the singlet states as

$$|s_1\rangle, |s_{\mathbf{8}_{aa}}\rangle, |s_{\mathbf{8}_{as}}\rangle, |s_{\mathbf{8}_{sa}}\rangle, |s_{\mathbf{8}_{aa}}\rangle, |s_{\mathbf{10}}\rangle, |s_{\overline{\mathbf{10}}}\rangle, |s_{\mathbf{27}}\rangle, \quad (2.2)$$

and similarly for the corresponding t -channel or u -channel bases.

The 4-gluon case of the potential (1.1) is

$$\begin{aligned} \underline{V}(\mathbf{b}_1, \mathbf{b}_2, \mathbf{b}_3, \mathbf{b}_4) = & -\frac{i}{8} \left\{ (2\hat{q}_{\text{Adj}} - \hat{q}_{12}) [(\mathbf{b}_1 - \mathbf{b}_2)^2 + (\mathbf{b}_3 - \mathbf{b}_4)^2] \right. \\ & + (2\hat{q}_{\text{Adj}} - \hat{q}_{13}) [(\mathbf{b}_1 - \mathbf{b}_3)^2 + (\mathbf{b}_2 - \mathbf{b}_4)^2] \\ & \left. + (2\hat{q}_{\text{Adj}} - \hat{q}_{14}) [(\mathbf{b}_1 - \mathbf{b}_4)^2 + (\mathbf{b}_2 - \mathbf{b}_3)^2] \right\}, \quad (2.3) \end{aligned}$$

where “Adj” means adjoint representation. Let the particle labels 1, 2, 3, 4 here correspond to the A, B, C, D of fig. 2. Then the s -channel basis (2.2) diagonalizes \hat{q}_{12} , since the R in fig.

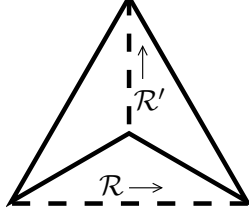


FIG. 4: A diagram representing (up to normalization and sign conventions) the overlap $\langle s_{\mathcal{R}}|t_{\mathcal{R}'}\rangle$, where solid lines represent the adjoint representations for each of our 4 gluons. [It also represents the overlap $\langle s_{\mathcal{R}}|u_{\mathcal{R}'}\rangle$, depending on how the 4 solid lines are identified with the particles ABCD of fig. 2.] When supplemented as necessary by the filled or open circles of fig. 3 in the case that \mathcal{R} or \mathcal{R}' is an adjoint representation, these diagrams are equivalent to those appearing in ref. [20]. The arrows shown above for \mathcal{R} and \mathcal{R}' are only relevant to the convention for distinguishing $\mathbf{10}$ vs. $\overline{\mathbf{10}}$ or $\mathbf{8}_{as}$ vs. $\mathbf{8}_{sa}$ in this diagram when comparing to ref. [20].

$\langle s_{\mathcal{R}} t_{\mathcal{R}'}\rangle$	$\mathbf{1}$	$\mathbf{8}_{aa}$	$\mathbf{8}_{as}$	$\mathbf{8}_{sa}$	$\mathbf{8}_{ss}$	$\mathbf{10}$	$\overline{\mathbf{10}}$	$\mathbf{27}$	conversion to $\langle s_{\mathcal{R}} u_{\mathcal{R}'}\rangle$
$\mathbf{1}$	$\frac{1}{8}$	$\frac{1}{2\sqrt{2}}$	0	0	$\frac{1}{2\sqrt{2}}$	$\frac{\sqrt{5}}{4\sqrt{2}}$	$\frac{\sqrt{5}}{4\sqrt{2}}$	$\frac{3\sqrt{3}}{8}$	+
$\mathbf{8}_{aa}$	$\frac{1}{2\sqrt{2}}$	$\frac{1}{2}$	0	0	$\frac{1}{2}$	0	0	$-\frac{\sqrt{3}}{2\sqrt{2}}$	-
$\mathbf{8}_{as}$	0	0	$-\frac{1}{2}$	$\frac{1}{2}$	0	$-\frac{1}{2}$	$\frac{1}{2}$	0	+
$\mathbf{8}_{sa}$	0	0	$\frac{1}{2}$	$-\frac{1}{2}$	0	$-\frac{1}{2}$	$\frac{1}{2}$	0	-
$\mathbf{8}_{ss}$	$\frac{1}{2\sqrt{2}}$	$\frac{1}{2}$	0	0	$-\frac{3}{10}$	$-\frac{1}{\sqrt{5}}$	$-\frac{1}{\sqrt{5}}$	$\frac{3\sqrt{3}}{10\sqrt{2}}$	+
$\mathbf{10}$	$\frac{\sqrt{5}}{4\sqrt{2}}$	0	$-\frac{1}{2}$	$-\frac{1}{2}$	$-\frac{1}{\sqrt{5}}$	$\frac{1}{4}$	$\frac{1}{4}$	$-\frac{\sqrt{3}}{4\sqrt{10}}$	-
$\overline{\mathbf{10}}$	$\frac{\sqrt{5}}{4\sqrt{2}}$	0	$\frac{1}{2}$	$\frac{1}{2}$	$-\frac{1}{\sqrt{5}}$	$\frac{1}{4}$	$\frac{1}{4}$	$-\frac{\sqrt{3}}{4\sqrt{10}}$	-
$\mathbf{27}$	$\frac{3\sqrt{3}}{8}$	$-\frac{\sqrt{3}}{2\sqrt{2}}$	0	0	$\frac{3\sqrt{3}}{10\sqrt{2}}$	$-\frac{\sqrt{3}}{4\sqrt{10}}$	$-\frac{\sqrt{3}}{4\sqrt{10}}$	$\frac{7}{40}$	+

TABLE I: Normalized st -channel overlaps $\langle s_{\mathcal{R}}|t_{\mathcal{R}'}\rangle$ of SU(3) singlets of four adjoint particles, where row labels indicate \mathcal{R} and column labels indicate \mathcal{R}' . Conversion to the corresponding su -channel overlaps $\langle s_{\mathcal{R}}|u_{\mathcal{R}'}\rangle$ is given by multiplying each row of $\langle s|t\rangle$ by the sign shown in the last column above.

a $|t_{\mathcal{R}'}\rangle$ would negate the corresponding column. So table I corresponds to a specific choice of sign conventions for the definition of the basis states.

The coefficients $\langle s_{\mathcal{R}}|u_{\mathcal{R}'}\rangle$ giving the transformation from the u -basis to the s -basis may now be obtained by swapping the labeling of particles C and D in fig. 2 to interchange t channel with u channel. Specifically, we'll define our u channel singlet states (including sign convention) by⁶

$$|u_{\mathcal{R}}\rangle \equiv |t_{\mathcal{R}}\rangle \text{ with } C \leftrightarrow D. \quad (2.9)$$

⁶ We could have alternatively constructed a definition based on $A \leftrightarrow B$, which would differ only by sign conventions from (2.9) and in the end would produce the same result for the \hat{q}_{14} of (2.6).

Then

$$\langle s_{\mathcal{R}}|u_{\mathcal{R}'}\rangle = \langle s_{\mathcal{R}}|\left(|t_{\mathcal{R}'}\rangle \text{ with } C\leftrightarrow D\right) = \left(\langle s_{\mathcal{R}}| \text{ with } C\leftrightarrow D\right)|t_{\mathcal{R}'}\rangle. \quad (2.10)$$

This corresponds to constructing $\langle s|u\rangle$ from $\langle s|t\rangle$ by negating those rows of table I where C and D are combined anti-symmetrically in $|s_{\mathcal{R}}\rangle$. According to (2.1), that's $\mathcal{R} = \mathbf{8}_{aa}, \mathbf{8}_{sa}, \mathbf{10}$ and $\overline{\mathbf{10}}$. We show the signs corresponding to this conversion in the last column of table I.

B. Block Diagonalization with Permutation Symmetries

Because the four representations we are combining into singlets are identical (four adjoints), there are certain permutation symmetries of ABCD that can be used to simultaneously block-diagonalize $\langle s|t\rangle$ and $\langle s|u\rangle$ and so reduce the number of singlet states that need be considered. Specifically, consider the channel-preserving permutations of ABCD that simultaneously map s -channel to s -channel, t -channel to t -channel, and u -channel to u -channel. From fig. 2, these are the symmetries of the rectangle one could draw connecting the labels ABCD shown in each of those diagrams. That is, there are two reflection symmetries

$$\sigma_1 : ABCD \leftrightarrow BADC, \quad \sigma_2 : ABCD \leftrightarrow CDAB, \quad (2.11a)$$

and the 180° rotation symmetry

$$\sigma_3 : ABCD \leftrightarrow DCBA. \quad (2.11b)$$

The symmetry group of the rectangle (known as D_2) is equivalent to $Z_2 \otimes Z_2$, where any two of the three symmetries (2.11) may be thought of as the two generators. In each channel, it will be useful to choose a new basis for our singlet states, having definite charge $(\sigma_1, \sigma_2, \sigma_3) = (\pm_1, \pm_2, \pm_3)$ under all three symmetries (2.11). That's slightly redundant, since $\sigma_1\sigma_2\sigma_3$ is the identity transformation and so $\sigma_1\sigma_2\sigma_3 = +1$. But the redundancy is useful for seeing a simple relation between charges in different channels: Consider $ABCD \rightarrow ACBD$, which changes s -channel to t -channel, and similarly $ABCD \rightarrow ADBC$ for s -channel to u -channel. Their actions on (2.11) give

$$\begin{aligned} (\sigma_1, \sigma_2, \sigma_3) = (\sigma_1^s, \sigma_2^s, \sigma_3^s) \text{ in } s\text{-channel construction} \\ \longrightarrow \begin{cases} (\sigma_1, \sigma_2, \sigma_3) = (\sigma_2^s, \sigma_1^s, \sigma_3^s) \text{ in } t\text{-channel construction;} \\ (\sigma_1, \sigma_2, \sigma_3) = (\sigma_2^s, \sigma_3^s, \sigma_1^s) \text{ in } u\text{-channel construction.} \end{cases} \quad (2.12) \end{aligned}$$

For each channel, table II lists $(\sigma_1, \sigma_2, \sigma_3)$ eigenstates and values.

Two states $|s_{\mathcal{R}}\rangle$ and $|t_{\mathcal{R}'}\rangle$ must have zero overlap $\langle s_{\mathcal{R}}|t_{\mathcal{R}'}\rangle$ if their charges $(\sigma_1, \sigma_2, \sigma_3)$ are different, and similarly for $|s_{\mathcal{R}}\rangle, |u_{\mathcal{R}'}\rangle$, and $\langle s_{\mathcal{R}}|u_{\mathcal{R}'}\rangle$. That means that the first five rows of table II do not mix with the last three rows, when one considers combining interactions mediated by different channels. Specifically, the forms (2.4) and (2.6) of \hat{q}_{12} , \hat{q}_{13} , and \hat{q}_{14} then imply that the 4-particle potential (2.3) block diagonalizes into 5×5 and 3×3 blocks corresponding to the first five rows and last three rows of table II. We will now see that our application lies within the 5×5 block, and so we may ignore the 3×3 block.

singlet state (channel $ch = s, t, \text{ or } u$)	$(\sigma_1, \sigma_2, \sigma_3)$		
	s -channel	t -channel	u -channel
$ \text{ch}_1\rangle$			
$ \text{ch}_{\mathbf{8}_{aa}}\rangle$			
$ \text{ch}_{\mathbf{8}_{ss}}\rangle$	(+, +, +)	(+, +, +)	(+, +, +)
$\frac{1}{\sqrt{2}}(\text{ch}_{\mathbf{10}}\rangle + \text{ch}_{\overline{\mathbf{10}}}\rangle)$			
$ \text{ch}_{\mathbf{27}}\rangle$			
$\frac{1}{\sqrt{2}}(\text{ch}_{\mathbf{8}_{as}}\rangle + \text{ch}_{\mathbf{8}_{sa}}\rangle)$	(-, +, -)	(+, -, -)	(+, -, -)
$\frac{1}{\sqrt{2}}(\text{ch}_{\mathbf{8}_{as}}\rangle - \text{ch}_{\mathbf{8}_{sa}}\rangle)$	(-, -, +)	(-, -, +)	(-, +, -)
$\frac{1}{\sqrt{2}}(\text{ch}_{\mathbf{10}}\rangle - \text{ch}_{\overline{\mathbf{10}}}\rangle)$	(+, -, -)	(-, +, -)	(-, -, +)

TABLE II: For each channel, the signs $(\sigma_1, \sigma_2, \sigma_3)$ of the singlet states under the three channel-preserving permutations ($ABCD \leftrightarrow BADC, ABCD \leftrightarrow CDBA, ABCD \leftrightarrow DCBA$).

C. Our application is a 5×5 problem

Consider an interference diagram such as fig. 1b for $g \rightarrow ggg$, which we used to introduce the need for the 4-gluon potential. We show the diagram again in fig. 5, now with the adjoint color indices of the gluons labeled, and with the regions of 3-particle evolution shaded in light blue (in addition to the 4-particle evolution shaded in gray). The important point about this diagram, true of any interference diagram for $g \rightarrow ggg$, is that 3-gluon vertices are associated with color factors given by Lie algebra structure constants f_{abc} . In consequence, the three gluons during the first phase of evolution are in the color singlet state

$$f_{CDe}|CDe\rangle. \quad (2.13)$$

None of the interactions with the medium can change this (after medium averaging),⁷ and so the color state remains the same just before the second vertex in fig. 5. That vertex then splits e into AB with a color factor of f_{ABe} , which means the intermediate (gray-shaded) region of 4-gluon evolution starts in color state

$$f_{ABe}f_{CDe}|ABCD\rangle. \quad (2.14)$$

This corresponds to particles AB being combined anti-symmetrically into a color adjoint state $f_{ABe}|AB\rangle$ and particles CD being similarly combined anti-symmetrically into a color adjoint state $f_{CDe}|CD\rangle$, and then an overall 4-gluon color singlet made from combining the two pairs. That is, the initial state (2.14) for 4-gluon evolution is (once normalized) just

⁷ In more detail, there are two possible color singlet states of 3 gluons: the completely anti-symmetric color combination (2.13) and the completely symmetric one $d_{CDe}|CDe\rangle$, where d_{abc} is defined in terms of fundamental representation generators by $2 \text{tr}(\{T_F^a, T_F^b\}T_F^c)$. These two singlets correspond to combining two of the three gluons into either the $\mathbf{8}_a$ or $\mathbf{8}_s$ of (2.1). In either case, $\hat{q}_{12} = \hat{q}_3$ for a 3-particle color singlet, and similarly $\hat{q}_{23} = \hat{q}_1$ and $\hat{q}_{31} = \hat{q}_2$. So the potential (1.1) for 3 gluons is $V(\mathbf{b}_1, \mathbf{b}_2, \mathbf{b}_3) = -\frac{i}{8}\hat{q}_A[(\mathbf{b}_1 - \mathbf{b}_2)^2 + (\mathbf{b}_2 - \mathbf{b}_3)^2 + (\mathbf{b}_3 - \mathbf{b}_1)^2]$, which (unlike the 4-body potential) has no interesting color structure [9, 16]: it is the same for both 3-gluon color singlets and so does not induce any transitions between the two.

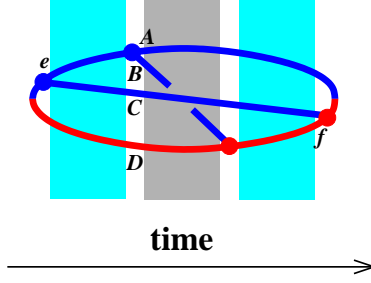


FIG. 5: Similar to fig. 1 but here showing labels for the adjoint color indices of all gluon lines.

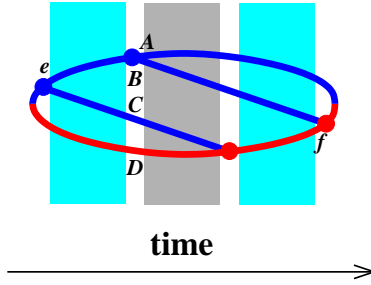


FIG. 6: Similar to fig. 5 but for a different $g \rightarrow ggg$ interference diagram.

what we've been calling $|s_{8_{aa}}\rangle$ in this paper. That places the 4-gluon evolution into the 5-dimensional subspace given by the first 5 rows of table II.

A similar argument working backward from the latest time in fig. 5 shows that the end color state of the 4-gluon evolution should be taken to be

$$|t_{8_{aa}}\rangle \propto f_{ACe}f_{BDe}|ABCD\rangle. \quad (2.15)$$

Which channel the end 4-gluon state is in compared to the initial 4-gluon state depends on the interference diagram. For example, for diagrams like fig. 6, both will be $|s_{8_{aa}}\rangle$. Regardless, everything will be in the sector of $(\sigma_1, \sigma_2, \sigma_3)=(+, +, +)$ singlet states.

The 5×5 unitary matrix of $\langle s|t \rangle$ overlaps in the $(\sigma_1, \sigma_2, \sigma_3)=(+, +, +)$ subspace is shown explicitly in table III.

III. THE EXPLICIT POTENTIAL AND CASIMIR SCALING

A. The 4-body potential

Restricting attention to the 5-dimensional subspace of relevant singlets, the 4-gluon potential is now given by (2.3) with

$$\underline{\hat{q}}_{12} = \underline{\hat{q}}_{\text{diag}} \equiv \begin{pmatrix} 0 & & & & \\ & \hat{q}_{\text{Adj}} & & & \\ & & \hat{q}_{\text{Adj}} & & \\ & & & \hat{q}_{10} & \\ & & & & \hat{q}_{27} \end{pmatrix}, \quad (3.1a)$$

$\langle s_{\mathcal{R}} t_{\mathcal{R}'}\rangle$	1	8_{aa}	8_{ss}	10+$\overline{10}$	27	conversion to $\langle s_{\mathcal{R}} u_{\mathcal{R}'}\rangle$
1	$\frac{1}{8}$	$\frac{1}{2\sqrt{2}}$	$\frac{1}{2\sqrt{2}}$	$\frac{\sqrt{5}}{4}$	$\frac{3\sqrt{3}}{8}$	+
8_{aa}	$\frac{1}{2\sqrt{2}}$	$\frac{1}{2}$	$\frac{1}{2}$	0	$-\frac{\sqrt{3}}{2\sqrt{2}}$	-
8_{ss}	$\frac{1}{2\sqrt{2}}$	$\frac{1}{2}$	$-\frac{3}{10}$	$-\frac{\sqrt{2}}{\sqrt{5}}$	$\frac{3\sqrt{3}}{10\sqrt{2}}$	+
10+$\overline{10}$	$\frac{\sqrt{5}}{4}$	0	$-\frac{\sqrt{2}}{\sqrt{5}}$	$\frac{1}{2}$	$-\frac{\sqrt{3}}{4\sqrt{5}}$	-
27	$\frac{3\sqrt{3}}{8}$	$-\frac{\sqrt{3}}{2\sqrt{2}}$	$\frac{3\sqrt{3}}{10\sqrt{2}}$	$-\frac{\sqrt{3}}{4\sqrt{5}}$	$\frac{7}{40}$	+

TABLE III: Normalized st -channel overlaps $\langle s_{\mathcal{R}}|t_{\mathcal{R}'}\rangle$ for the relevant subspace of SU(3) singlets of four adjoint particles. Here **10+ $\overline{10}$** is shorthand for the $\frac{1}{\sqrt{2}}(|\text{ch}_{10}\rangle + |\text{ch}_{\overline{10}}\rangle)$ state of table II. The last column shows how to convert to $\langle s_{\mathcal{R}}|u_{\mathcal{R}'}\rangle$ just as in table I.

$$\hat{q}_{13} = \underline{\langle s|t\rangle} \hat{q}_{\text{diag}} \underline{\langle s|t\rangle}^\dagger, \quad (3.1b)$$

and

$$\hat{q}_{14} = \underline{\langle s|u\rangle} \hat{q}_{\text{diag}} \underline{\langle s|u\rangle}^\dagger = \underline{P} \hat{q}_{13} \underline{P}, \quad (3.1c)$$

where $\underline{\langle s|t\rangle}$ is given by table III, and \underline{P} is a diagonal matrix composed of the signs in the last column of that table:

$$\underline{P} \equiv \begin{pmatrix} + & & & & \\ & - & & & \\ & & + & & \\ & & & - & \\ & & & & + \end{pmatrix}. \quad (3.1d)$$

B. An additional consistency condition

Ref. [16] showed that consistency of the harmonic oscillator (\hat{q}) approximation to the n -body potential requires that approximation to have the form (1.1) and so, in the 4-body case, requires (2.3). However, ref. [16] did not show the inverse: it did not prove that (1.1) is always consistent. ‘‘Consistency’’ here means that the n -body potential matches the $(n-1)$ -body potential in the special cases where two of the particles are in the same place (i.e. $\mathbf{b}_i=\mathbf{b}_j$ for some i and j). We’re now in a position to check this for the 4-gluon potential given by (2.3), (3.1), and table III. Consider the special case where $\mathbf{b}_3=\mathbf{b}_4$ in (2.3), giving

$$\underline{V}(\mathbf{b}_1, \mathbf{b}_2, \mathbf{b}_3, \mathbf{b}_3) = -\frac{i}{8} \left\{ (2\hat{q}_{\text{Adj}} - \hat{q}_{12})(\mathbf{b}_1 - \mathbf{b}_2)^2 + (4\hat{q}_{\text{Adj}} - \hat{q}_{13} - \hat{q}_{14})[(\mathbf{b}_1 - \mathbf{b}_3)^2 + (\mathbf{b}_2 - \mathbf{b}_3)^2] \right\}. \quad (3.2)$$

However, as in ref. [16], we may alternatively think of this situation as a *three*-particle problem by replacing coincident particles 3 and 4 above by a single particle with their combined color representation, i.e. by replacing $\hat{q}_3 \rightarrow \hat{q}_{34}$ in the formula for a 3-body particles potential.

Generically, the 3-body case of the n -body potential (1.1) is [9, 16]

$$\underline{V}(\mathbf{b}_1, \mathbf{b}_2, \mathbf{b}_3) = -\frac{i}{8} \left\{ (\hat{q}_1 + \hat{q}_2 - \hat{q}_3)(\mathbf{b}_1 - \mathbf{b}_2)^2 + (\hat{q}_2 + \hat{q}_3 - \hat{q}_1)(\mathbf{b}_2 - \mathbf{b}_3)^2 + (\hat{q}_3 + \hat{q}_1 - \hat{q}_2)(\mathbf{b}_3 - \mathbf{b}_1)^2 \right\}, \quad (3.3)$$

where the fact that the potential is for an overall 3-body color singlet has been used to replace the \hat{q}_{12} of (1.1) by \hat{q}_3 in (3.3), with similar replacements for \hat{q}_{13} and \hat{q}_{23} . Consistency of (3.2) and (3.3) then implies that we must have

$$\underline{V}(\mathbf{b}_1, \mathbf{b}_2, \mathbf{b}_3, \mathbf{b}_3) = \left[V(\mathbf{b}_1, \mathbf{b}_2, \mathbf{b}_3) \text{ with } \hat{q}_3 \rightarrow \hat{q}_{34} \right]. \quad (3.4)$$

Ref. [16] focused on the consistency of what, in the case of (3.2), would be the $(\mathbf{b}_1 - \mathbf{b}_2)^2$ term. Appropriately generalized, that comparison was the basis for how the n -body potential (1.1) was determined. Here, let's also check the consistency of the *other* terms in (3.2). Comparing (3.2) to (3.3) via (3.4), we see that full consistency of the 4-gluon potential is achieved if and only if additionally

$$4\hat{q}_{\text{Adj}} - \hat{q}_{13} - \hat{q}_{14} = \hat{q}_{34}. \quad (3.5)$$

$\hat{q}_{34} = \hat{q}_{12}$ since the 4 gluons form a color singlet, and so we can rewrite the consistency condition (3.5) as

$$\hat{q}_{12} + \hat{q}_{13} + \hat{q}_{14} = 4\hat{q}_{\text{Adj}}. \quad (3.6)$$

This same condition could alternatively be derived by looking at the special case $\mathbf{b}_2 = \mathbf{b}_3 = \mathbf{b}_4$ of the 4-gluon potential (2.3),

$$\underline{V}(\mathbf{b}_1, \mathbf{b}_2, \mathbf{b}_2, \mathbf{b}_2) = -\frac{i}{8} (6\hat{q}_{\text{Adj}} - \hat{q}_{12} - \hat{q}_{13} - \hat{q}_{14})(\mathbf{b}_1 - \mathbf{b}_2)^2 \}. \quad (3.7)$$

By overall color neutrality, the combination of the coincident particles 2, 3, and 4 must be in the adjoint representation, and so (3.7) must match up with the 2-gluon potential $V(\mathbf{b}_1, \mathbf{b}_2) = -\frac{i}{8}(2\hat{q}_{\text{Adj}})(\mathbf{b}_1 - \mathbf{b}_2)^2$. That matching also gives (3.6).

C. Consistency implies Casimir Scaling of \hat{q}

Using the explicit formulas of (3.1) and table III, we find that (3.6) is satisfied only if the \hat{q}_R for the three non-trivial representations $R = \mathbf{8}$, $\mathbf{10}$, and $\mathbf{27}$ appearing in our analysis are related by Casimir scaling. Namely, consistency requires

$$\hat{q}_{\mathbf{10}} = \frac{C_{\mathbf{10}}}{C_{\text{Adj}}} \hat{q}_{\text{Adj}} = 2\hat{q}_{\text{Adj}} \quad \text{and} \quad \hat{q}_{\mathbf{27}} = \frac{C_{\mathbf{27}}}{C_{\text{Adj}}} \hat{q}_{\text{Adj}} = \frac{8}{3}\hat{q}_{\text{Adj}}. \quad (3.8)$$

We speculate that there is a general argument that applies to other representations as well, but in this paper we focus only on the application to 4-gluon potentials.

Casimir scaling implies that

$$\hat{q}_{ij}^2 = \frac{C_{ij}}{C_{\text{Adj}}} \hat{q}_{\text{Adj}} = \frac{(\mathbb{T}_i + \mathbb{T}_j)^2}{C_{\text{Adj}}} \hat{q}_{\text{Adj}} = \frac{C_i + 2\mathbb{T}_i \cdot \mathbb{T}_j + C_j}{C_{\text{Adj}}} \hat{q}_{\text{Adj}}, \quad (3.9)$$

where (following the notation of ref. [16]) \mathbb{T}_i^a are the color generators acting on particle i , and $\underline{\mathbb{T}}_i \cdot \underline{\mathbb{T}}_j \equiv \mathbb{T}_i^a \cdot \mathbb{T}_j^a$. The 4-gluon potential (2.3) can then be rewritten as

$$\begin{aligned} \underline{V}(\mathbf{b}_1, \mathbf{b}_2, \mathbf{b}_3, \mathbf{b}_4) = \frac{i\hat{q}_{\text{Adj}}}{4} \left\{ \frac{\underline{\mathbb{T}}_1 \cdot \underline{\mathbb{T}}_2}{C_{\text{Adj}}} [(\mathbf{b}_1 - \mathbf{b}_2)^2 + (\mathbf{b}_3 - \mathbf{b}_4)^2] \right. \\ \left. + \frac{\underline{\mathbb{T}}_1 \cdot \underline{\mathbb{T}}_3}{C_{\text{Adj}}} [(\mathbf{b}_1 - \mathbf{b}_3)^2 + (\mathbf{b}_2 - \mathbf{b}_4)^2] \right. \\ \left. + \frac{\underline{\mathbb{T}}_1 \cdot \underline{\mathbb{T}}_4}{C_{\text{Adj}}} [(\mathbf{b}_1 - \mathbf{b}_4)^2 + (\mathbf{b}_2 - \mathbf{b}_3)^2] \right\}, \end{aligned} \quad (3.10)$$

which has the same form as the weakly-coupled plasma result discussed in [16] but here is now a feature for \hat{q} approximations in strongly-coupled plasmas as well.

We can relate the $\underline{\mathbb{T}}_i \cdot \underline{\mathbb{T}}_j$ of (3.10) back to (3.1) for the \hat{q}_{ij} via

$$\frac{\underline{\mathbb{T}}_i \cdot \underline{\mathbb{T}}_j}{C_{\text{Adj}}} = \frac{\hat{q}_{ij}}{2\hat{q}_{\text{Adj}}} - \underline{\mathbb{1}}. \quad (3.11)$$

This yields explicit results

$$\frac{\underline{\mathbb{T}}_1 \cdot \underline{\mathbb{T}}_2}{C_{\text{Adj}}} = -\underline{S}, \quad \frac{\underline{\mathbb{T}}_1 \cdot \underline{\mathbb{T}}_3}{C_{\text{Adj}}} = \frac{1}{2}(\underline{S} - \underline{\mathbb{1}}) - \underline{T}, \quad \frac{\underline{\mathbb{T}}_1 \cdot \underline{\mathbb{T}}_4}{C_{\text{Adj}}} = \frac{1}{2}(\underline{S} - \underline{\mathbb{1}}) + \underline{T}, \quad (3.12a)$$

where

$$\underline{S} \equiv \begin{pmatrix} 1 & & & & \\ & \frac{1}{2} & & & \\ & & \frac{1}{2} & & \\ & & & 0 & \\ & & & & -\frac{1}{3} \end{pmatrix}, \quad \underline{T} \equiv \begin{pmatrix} 0 & \frac{1}{2\sqrt{2}} & 0 & 0 & 0 \\ \frac{1}{2\sqrt{2}} & 0 & \frac{1}{4} & 0 & \frac{1}{2\sqrt{6}} \\ 0 & \frac{1}{4} & 0 & \frac{1}{\sqrt{10}} & 0 \\ 0 & 0 & \frac{1}{\sqrt{10}} & 0 & \frac{1}{\sqrt{15}} \\ 0 & \frac{1}{2\sqrt{6}} & 0 & \frac{1}{\sqrt{15}} & 0 \end{pmatrix}. \quad (3.12b)$$

IV. REDUCTION OF 4-BODY TO EFFECTIVE 2-BODY PROBLEM

For applications to overlapping formation times, ref. [9] showed that symmetries and conservation laws could be used to mathematically reduce the 4-body evolution problem to an effective 2-body evolution problem.⁸ In the notation of ref. [9], we can rewrite differences of $(\mathbf{b}_1, \mathbf{b}_2, \mathbf{b}_3, \mathbf{b}_4)$ in terms of $(\mathbf{C}_{12}, \mathbf{C}_{34})$ with

$$\mathbf{C}_{ij} \equiv \frac{\mathbf{b}_i - \mathbf{b}_j}{x_i + x_j}, \quad (4.1)$$

where x_i is the longitudinal momentum fraction of particle i in figs. 5 or 6, relative to the longitudinal momentum of the initial gluon that started the $g \rightarrow ggg$ double splitting process. The x_i are defined with a sign convention for particles in the conjugate amplitude

⁸ See in particular section III of ref. [9].

so that $x_1 + x_2 + x_3 + x_4 = 0$. The relations are⁹

$$\mathbf{b}_1 - \mathbf{b}_2 = (x_1 + x_2)\mathbf{C}_{12}, \quad (4.2a)$$

$$\mathbf{b}_1 - \mathbf{b}_3 = x_2\mathbf{C}_{12} - x_4\mathbf{C}_{34}, \quad (4.2b)$$

$$\mathbf{b}_1 - \mathbf{b}_4 = x_2\mathbf{C}_{12} + x_3\mathbf{C}_{34}, \quad (4.2c)$$

$$\mathbf{b}_2 - \mathbf{b}_3 = -x_1\mathbf{C}_{12} - x_4\mathbf{C}_{34}, \quad (4.2d)$$

$$\mathbf{b}_2 - \mathbf{b}_4 = -x_1\mathbf{C}_{12} + x_3\mathbf{C}_{34}, \quad (4.2e)$$

$$\mathbf{b}_3 - \mathbf{b}_4 = (x_3 + x_4)\mathbf{C}_{34}. \quad (4.2f)$$

Eqs. (3.10) and (3.12a) then give

$$\begin{aligned} \underline{V}(\mathbf{C}_{12}, \mathbf{C}_{34}) = & -\frac{i}{4}\hat{q}_{\text{Adj}} \left\{ (x_1^2 + 2x_1x_2\underline{S} + x_2^2)C_{12}^2 + (x_3^2 + 2x_3x_4\underline{S} + x_4^2)C_{34}^2 \right. \\ & \left. + 2\left[\frac{1}{2}(x_1 - x_2)(x_3 - x_4)(\underline{S} - 1) - (x_1 + x_2)(x_3 + x_4)\underline{T}\right]\mathbf{C}_{12} \cdot \mathbf{C}_{34} \right\}. \end{aligned} \quad (4.3a)$$

Ref. [9] shows that the Schrödinger-like problem describing 4-particle evolution has Hamiltonian¹⁰

$$\underline{H} = \frac{P_{12}^2}{2x_1x_2(x_1+x_2)E} + \frac{P_{34}^2}{2x_3x_4(x_3+x_4)E} + \underline{V}(\mathbf{C}_{12}, \mathbf{C}_{34}), \quad (4.3b)$$

except that the potential $V(\mathbf{C}_{12}, \mathbf{C}_{34})$ there has been replaced by a 5×5 matrix-valued potential here, as indicated by the underlining above. \mathbf{P}_{12} and \mathbf{P}_{34} are the momenta conjugate to \mathbf{C}_{12} and \mathbf{C}_{34} , and E is the energy of the initial gluon in the $g \rightarrow ggg$ double splitting process.

Due to rotational invariance, the harmonic oscillator potential (4.3a) does not mix the x -components of $(\mathbf{C}_{12}, \mathbf{C}_{34})$ with the y -components, so the problem of solving the system (4.3b) can be reduced to solving a system of two coupled *one*-dimensional oscillators. Each of those one-dimensional problems has the form of (1.2),

$$\underline{H} = \frac{p_1^2}{2m_1} + \frac{p_2^2}{2m_2} + \frac{1}{2} \begin{pmatrix} q_1 \\ q_2 \end{pmatrix}^\top \begin{pmatrix} \underline{a} & \underline{b} \\ \underline{b} & \underline{c} \end{pmatrix} \begin{pmatrix} q_1 \\ q_2 \end{pmatrix}, \quad (4.4)$$

with

$$m_1 = x_1x_2(x_1 + x_2)E, \quad (4.5)$$

$$m_2 = x_3x_4(x_3 + x_4)E, \quad (4.6)$$

and

$$\underline{a} = -\frac{i}{2}\hat{q}_{\text{Adj}}(x_1^2 + 2x_1x_2\underline{S} + x_2^2), \quad (4.7)$$

$$\underline{b} = -\frac{i}{2}\hat{q}_{\text{Adj}}\left[\frac{1}{2}(x_1 - x_2)(x_3 - x_4)(\underline{S} - 1) - (x_1 + x_2)(x_3 + x_4)\underline{T}\right], \quad (4.8)$$

$$\underline{c} = -\frac{i}{2}\hat{q}_{\text{Adj}}(x_3^2 + 2x_3x_4\underline{S} + x_4^2). \quad (4.9)$$

⁹ Eqs. (5.14) of ref. [9].

¹⁰ Specifically, (4.3b) here is the Hamiltonian corresponding to the Lagrangian displayed in eqs. (5.15–16) of ref. [9].

The calculations [9] of overlapping splitting make use of the propagator $G(\mathbf{C}'_{12}, \mathbf{C}'_{34}, t; \mathbf{C}_{12}, \mathbf{C}_{34}, 0)$ for 4-particle evolution. Recall from section IIC that the 4-particle evolution starts with the singlet state $|\text{ch}_{\mathbf{8}_{aa}}\rangle$ in some channel ($\text{ch} = s, t, \text{ or } u$, depending on how we label the particles) and similarly ends with the singlet state $|\text{ch}'_{\mathbf{8}_{aa}}\rangle$ in some channel ($\text{ch}' = s, t, \text{ or } u$, depending on the interference diagram). The relevant propagator matrix elements for the 2-dimensional problem (4.3b) can then be written in terms of the 1-dimensional version (4.4) as

$$\begin{aligned} \langle \text{ch}'_{\mathbf{8}_{aa}} | \underline{G}(\mathbf{C}'_{12}, \mathbf{C}'_{34}, t; \mathbf{C}_{12}, \mathbf{C}_{34}, 0) | \text{ch}_{\mathbf{8}_{aa}} \rangle = \\ \langle \text{ch}'_{\mathbf{8}_{aa}} | \underline{G}_{(1)}(C'_{12,x}, C'_{34,x}, t; C_{12,x}, C_{34,x}, 0) | \text{ch}_{\mathbf{8}_{aa}} \rangle \\ \times \langle \text{ch}'_{\mathbf{8}_{aa}} | \underline{G}_{(1)}(C'_{12,y}, C'_{34,y}, t; C_{12,y}, C_{34,y}, 0) | \text{ch}_{\mathbf{8}_{aa}} \rangle. \end{aligned} \quad (4.10)$$

In the s -channel basis ($|s_1\rangle, |s_{\mathbf{8}_{aa}}\rangle, |s_{\mathbf{8}_{ss}}\rangle, |s_{\mathbf{10}+\overline{\mathbf{10}}}\rangle, |s_{\mathbf{27}}\rangle$) used for our matrices in (3.12b),

$$|s_{\mathbf{8}_{aa}}\rangle \rightarrow \begin{pmatrix} 0 \\ 1 \\ 0 \\ 0 \\ 0 \\ 0 \end{pmatrix} \quad \text{and} \quad |t_{\mathbf{8}_{aa}}\rangle \rightarrow \underline{\langle s|t \rangle} \begin{pmatrix} 0 \\ 1 \\ 0 \\ 0 \\ 0 \\ 0 \end{pmatrix} = \begin{pmatrix} \frac{1}{2\sqrt{2}} \\ \frac{1}{2} \\ \frac{1}{2} \\ 0 \\ -\frac{\sqrt{3}}{2\sqrt{2}} \\ 0 \end{pmatrix}. \quad (4.11)$$

We will explain in the conclusion why the color matrix structure of the propagator \underline{G} creates a much more difficult problem for numerical calculations of overlapping splittings than for the large- N_c case [9].

V. SU(N) AND RECOVERING THE LARGE- N LIMIT

We will now generalize the preceding results from SU(3) to SU(N), with the goal of studying how the (simpler) large- N formalism for earlier calculations [9–12] of overlapping formation time effects is recovered as $N \rightarrow \infty$. From here on, we refer to the number of colors N_c as simply N to make formulas more compact and easy to read.

A. SU(N) results

An interesting feature of SU(N) for $N > 3$ is that one more irreducible representation appears in the tensor product $\text{Adj} \otimes \text{Adj}$ than for SU(3). Reassuringly, we will find that the limit $N \rightarrow 3$ of the potential nonetheless smoothly approaches the SU(3) case. In terms of Young Tableaux, the tensor product $\text{Adj} \otimes \text{Adj}$ is

$$(5.1)$$

$\langle s_{\mathcal{R}} t_{\mathcal{R}'}\rangle$	1	“ 8 ” _{aa}	“ 8 ” _{ss}	“ 10 + $\overline{\mathbf{10}}$ ”	“ 27 ”	“ 0 ”	conversion to $\langle s_{\mathcal{R}} u_{\mathcal{R}'}\rangle$
1	$\frac{1}{N^2-1}$	$\sqrt{\frac{1}{N^2-1}}$	$\sqrt{\frac{1}{N^2-1}}$	$\sqrt{\frac{N^2-4}{2(N^2-1)}}$	$\frac{N}{2(N+1)}\sqrt{\frac{N+3}{N-1}}$	$\frac{N}{2(N-1)}\sqrt{\frac{N-3}{N+1}}$	+
“ 8 ” _{aa}		$\frac{1}{2}$	$\frac{1}{2}$	0	$-\frac{1}{2}\sqrt{\frac{N+3}{N+1}}$	$\frac{1}{2}\sqrt{\frac{N-3}{N-1}}$	-
“ 8 ” _{ss}			$\frac{N^2-12}{2(N^2-4)}$	$-\sqrt{\frac{2}{N^2-4}}$	$\frac{N}{2(N+2)}\sqrt{\frac{N+3}{N+1}}$	$-\frac{N}{2(N-2)}\sqrt{\frac{N-3}{N-1}}$	+
“ 10 + $\overline{\mathbf{10}}$ ”		(symmetric)		$\frac{1}{2}$	$-\sqrt{\frac{(N-2)(N+3)}{8(N+1)(N+2)}}$	$-\sqrt{\frac{(N+2)(N-3)}{8(N-1)(N-2)}}$	-
“ 27 ”					$\frac{N^2+N+2}{4(N+1)(N+2)}$	$\frac{1}{4}\sqrt{\frac{N^2-9}{N^2-1}}$	+
“ 0 ”			(symmetric)			$\frac{N^2-N+2}{4(N-1)(N-2)}$	+

TABLE IV: The $SU(N)$ generalization of table III. Since the table is symmetric, we have not bothered to show the entries below the main diagonal.

with corresponding dimensions

$$\begin{aligned}
(N^2-1)\otimes(N^2-1) = & 1_s \oplus (N^2-1)_a \oplus (N^2-1)_s \oplus \left(\frac{(N^2-4)(N^2-1)}{4}\right)_a \oplus \left(\frac{(N^2-4)(N^2-1)}{4}\right)_a \\
& \oplus \left(\frac{N^2(N-1)(N+3)}{4}\right)_s \oplus \left(\frac{N^2(N+1)(N-3)}{4}\right)_s. \quad (5.2)
\end{aligned}$$

For the sake of easy comparison to previous $SU(3)$ results, we’ll refer to these representations by their $N=3$ dimensions but use scare quotes as a reminder that we’re really considering $N > 3$:

$$\text{“8”} \otimes \text{“8”} = \mathbf{1}_s \oplus \text{“8”}_a \oplus \text{“8”}_s \oplus \text{“10”}_a \oplus \overline{\text{“10”}}_a \oplus \text{“27”}_s \oplus \text{“0”}_s. \quad (5.3)$$

The extra irreducible representation for $N>3$ is the one labeled “**0**” above, and the corresponding Young Tableaux in (5.1) is illegal for $SU(3)$. However, a first point of reassurance concerning using $N>3$ results to study the transition from $N\rightarrow\infty$ to $N=3$ is that the dimension of this unwanted representation shrinks to zero as $N\rightarrow 3$.

In appendix A, we discuss explicit constructions of (i) the irreducible representations in the decomposition (5.3) and (ii) the corresponding 4-gluon singlet states. Similar to the $|\text{ch}_{\mathbf{27}}\rangle$ of table II, singlets $|\text{ch}_{\mathbf{0}}\rangle$ based on the new representation “**0**” also have $(\sigma_1, \sigma_2, \sigma_3) = (+, +, +)$ and so mix with the rest of the $(+, +, +)$ sector. For $N > 3$, we therefore need to represent the potential using 6×6 matrices instead of 5×5 ones. Table IV presents the corresponding table of $\langle s|t\rangle$ matrix elements, whose computation is also discussed in appendix A. Alternatively, the entries not involving “**0**” may be extracted from Sjodahl and Thorén [20],¹¹ and the “**0**” entries could then be determined from unitarity of $\langle s|t\rangle$.

In the limit $N\rightarrow 3$, the 4-gluon singlets $|\text{ch}_{\mathbf{0}}\rangle$ constructed from the “**0**” representation no longer mix in table IV with any of the other singlets and so will completely decouple

¹¹ The normalization conversion is the same as that of footnote 5, here using the $SU(N)$ dimensions (5.2). Then one must take the same combination of “**10**” and “ $\overline{\mathbf{10}}$ ” used to go from table I to table III.

from calculations of overlapping formation time effects:

$$\begin{array}{ccc}
 \boxed{\text{Table IV}} & \xrightarrow{N=3} & \boxed{\begin{array}{c|c} \text{Table III} & \begin{array}{c} 0 \\ 0 \\ 0 \\ 0 \\ 0 \end{array} \\ \hline 0 & 0 & 0 & 0 & 0 & 1 \end{array}}. \quad (5.4)
 \end{array}$$

This is the reason that $SU(N)$ results for our application will smoothly approach the $SU(3)$ result as $N \rightarrow 3$.

Note that if we were interested in $SU(2)$ gauge theory, the situation would be more complicated. For $SU(2)$, the decomposition is $\text{Adj} \otimes \text{Adj} = \mathbf{3} \otimes \mathbf{3} = \mathbf{1}_s \oplus \mathbf{3}_a \oplus \mathbf{5}_s$, which in our $SU(3)$ -based notation (5.3) corresponds to what we've called $\mathbf{1}_s \oplus \mathbf{8}_a \oplus \mathbf{27}_s$. But the unwanted representations " $\mathbf{8}_s$ ", " $\mathbf{10} + \overline{\mathbf{10}}$ " and " $\mathbf{0}$ " in the $SU(2)$ case do not simply decouple if we set $N=2$ in table IV. Also, some of the entries involving those unwanted representations are infinite for $N=2$. Since our application of interest is $SU(3)$, we'll ignore the issue of whether (and how) one can interpolate our $N > 3$ results to $SU(2)$.

As for $SU(3)$, consistency requires Casimir scaling of \hat{q} , which gives

$$\hat{q}_{\text{diag}} = \frac{\hat{q}_{\text{Adj}}}{C_{\text{Adj}}} \left(\begin{array}{cccc|c} 0 & & & & \\ & C_{\text{Adj}} & & & \\ & & C_{\text{Adj}} & & \\ & & & C_{\mathbf{10}} & \\ \hline & & & & C_{\mathbf{27}} \\ & & & & C_{\mathbf{0}} \end{array} \right) = \hat{q}_{\text{Adj}} \left(\begin{array}{cccc|c} 0 & & & & \\ & 1 & & & \\ & & 1 & & \\ & & & 2 & \\ \hline & & & & 2 + \frac{2}{N} \\ & & & & 2 - \frac{2}{N} \end{array} \right). \quad (5.5)$$

The generalizations of the matrices \underline{S} and \underline{T} of (3.12b) are then found to be

$$\underline{S} \equiv \left(\begin{array}{cccc|c} 1 & & & & \\ & \frac{1}{2} & & & \\ & & \frac{1}{2} & & \\ & & & 0 & \\ \hline & & & & -\frac{1}{N} \\ & & & & \frac{1}{N} \end{array} \right) \quad (5.6a)$$

and

$$\underline{T} \equiv \left(\begin{array}{cccccc|c} 0 & \frac{1}{\sqrt{N^2-1}} & 0 & 0 & 0 & 0 & \\ \frac{1}{\sqrt{N^2-1}} & 0 & \frac{1}{4} & 0 & \frac{1}{2N} \sqrt{\frac{N+3}{N+1}} & \frac{1}{2N} \sqrt{\frac{N-3}{N-1}} & \\ 0 & \frac{1}{4} & 0 & \frac{1}{\sqrt{2(N^2-4)}} & 0 & 0 & \\ 0 & 0 & \frac{1}{\sqrt{2(N^2-4)}} & 0 & \tau_+ & \tau_- & \\ 0 & \frac{1}{2N} \sqrt{\frac{N+3}{N+1}} & 0 & \tau_+ & 0 & 0 & \\ \hline 0 & \frac{1}{2N} \sqrt{\frac{N-3}{N-1}} & 0 & \tau_- & 0 & 0 & \end{array} \right), \quad (5.6b)$$

where

$$\tau_{\pm} \equiv \frac{1}{2N} \sqrt{\frac{(N\mp 2)(N\pm 1)(N\pm 3)}{2(N\pm 2)}}. \quad (5.7)$$

B. The large- N limit

In the large- N limit, (5.6) becomes

$$\underline{S} \rightarrow \begin{pmatrix} 1 & & & & & \\ & \boxed{\begin{matrix} \frac{1}{2} & \\ & \frac{1}{2} \end{matrix}} & & & & \\ & & 0 & & & \\ & & & 0 & & \\ & & & & 0 & \\ & & & & & 0 \end{pmatrix}, \quad \underline{T} \equiv \begin{pmatrix} 0 & & & & & \\ & \boxed{\begin{matrix} 0 & \frac{1}{4} \\ \frac{1}{4} & 0 \end{matrix}} & & & & \\ & & 0 & \frac{1}{2\sqrt{2}} & \frac{1}{2\sqrt{2}} & \\ & & \frac{1}{2\sqrt{2}} & 0 & 0 & \\ & & \frac{1}{2\sqrt{2}} & 0 & 0 & \end{pmatrix}, \quad (5.8)$$

where the boxes highlight the subspace ($|s_{\text{Adj}_{\text{aa}}}\rangle, |s_{\text{Adj}_{\text{ss}}}\rangle$). We see that those two singlets decouple from all the others. Since this is the subspace that our initial 4-gluon state $|s_{\text{Adj}_{\text{aa}}}\rangle$ belongs to, we can reduce the 6×6 matrix problem to a 2×2 problem in the large N limit. The 4-body potential given by (3.10) and (3.12) is then

$$\begin{aligned} \underline{V}(\mathbf{b}_1, \mathbf{b}_2, \mathbf{b}_3, \mathbf{b}_4) = & -\frac{i\hat{q}_A}{8} \left\{ \begin{pmatrix} 1 & 0 \\ 0 & 1 \end{pmatrix} [(\mathbf{b}_1 - \mathbf{b}_2)^2 + (\mathbf{b}_3 - \mathbf{b}_4)^2] \right. \\ & + \frac{1}{2} \begin{pmatrix} 1 & 1 \\ 1 & 1 \end{pmatrix} [(\mathbf{b}_1 - \mathbf{b}_3)^2 + (\mathbf{b}_2 - \mathbf{b}_4)^2] \\ & \left. + \frac{1}{2} \begin{pmatrix} 1 & -1 \\ -1 & 1 \end{pmatrix} [(\mathbf{b}_1 - \mathbf{b}_4)^2 + (\mathbf{b}_2 - \mathbf{b}_3)^2] \right\}. \end{aligned} \quad (5.9)$$

This potential can be diagonalized in color-singlet space by switching basis to

$$|s_{\text{Adj}_{\pm}}\rangle \equiv \frac{1}{\sqrt{2}} (|s_{\text{Adj}_{\text{aa}}}\rangle \pm |s_{\text{Adj}_{\text{ss}}}\rangle), \quad (5.10)$$

with

$$V_+(\mathbf{b}_1, \mathbf{b}_2, \mathbf{b}_3, \mathbf{b}_4) = -\frac{i\hat{q}_A}{8} [(\mathbf{b}_1 - \mathbf{b}_2)^2 + (\mathbf{b}_2 - \mathbf{b}_4)^2 + (\mathbf{b}_4 - \mathbf{b}_3)^2 + (\mathbf{b}_3 - \mathbf{b}_1)^2], \quad (5.11a)$$

$$V_-(\mathbf{b}_1, \mathbf{b}_2, \mathbf{b}_3, \mathbf{b}_4) = -\frac{i\hat{q}_A}{8} [(\mathbf{b}_1 - \mathbf{b}_2)^2 + (\mathbf{b}_2 - \mathbf{b}_3)^2 + (\mathbf{b}_3 - \mathbf{b}_4)^2 + (\mathbf{b}_4 - \mathbf{b}_1)^2]. \quad (5.11b)$$

Eqs. (5.11) exactly match the two color routings used in previous large- N work on overlapping formation times [10] for the contribution of diagrams like fig. 6.

In contrast, previous large- N work [9] did *not* need to study two different color routings for diagrams like fig. 5. In terms of our analysis here, this happens because the 4-particle evolution in those diagrams starts with $|s_{\text{Adj}_{\text{aa}}}\rangle$ and ends with $\langle t_{\text{Adj}_{\text{aa}}}|$. Using table IV, the

large- N analog of the $SU(3)$ representation (4.11) of these states as vectors is

$$|s_{\text{Adj}_{\text{aa}}}\rangle \rightarrow \begin{pmatrix} 0 \\ 1 \\ 0 \\ 0 \\ 0 \\ 0 \end{pmatrix} \quad \text{and} \quad |t_{\text{Adj}_{\text{aa}}}\rangle \rightarrow \underline{\langle s|t\rangle} \begin{pmatrix} 0 \\ 1 \\ 0 \\ 0 \\ 0 \\ 0 \end{pmatrix} = \begin{pmatrix} 0 \\ \frac{1}{2} \\ \frac{1}{2} \\ 0 \\ -\frac{1}{2} \\ \frac{1}{2} \end{pmatrix}. \quad (5.12)$$

So, ending the evolution with $\langle t_{\text{Adj}_{\text{aa}}} |$ in fig. 5 automatically projects out just the V_+ potential (5.11a).¹²

VI. CONCLUSION

Calculations in the literature of the effect of overlapping formation times on in-medium shower development have resorted to either soft bremsstrahlung or large- N limits. Previous large- N calculations, that avoid soft-bremsstrahlung approximations, use propagators for 4-particle evolution in figs. 5 and 6 mathematically equivalent to the propagator for a system of two non-relativistic (and non-Hermitian) coupled harmonic oscillators. We’ve shown here that the large- N limit can be avoided at the cost of replacing the “spring constants” of that harmonic oscillator problem by constant 5×5 matrices, which have been explicitly derived in this paper for $g \rightarrow ggg$ processes. These constant matrices act on an internal color space of 4-gluon color singlets. Unfortunately, the two matrices \underline{S} and \underline{T} (3.12b) used in their construction (4.3) do not commute outside of the large- N limit, and so the harmonic oscillator problem (4.4) cannot be solved by straightforward diagonalization in color-singlet space. We do not know how to find a closed-form solution for this “harmonic oscillator” propagator. One could, of course, instead solve for the propagator numerically by solving the corresponding Schrödinger equation numerically, which would be

$$i\partial_t \underline{G}_{(1)}(q'_1, q'_2, t; q_1, q_2, 0) = \left[-\frac{\partial_{q'_1}^2}{2m_1} - \frac{\partial_{q'_2}^2}{2m_2} + \frac{1}{2} \begin{pmatrix} q_1 \\ q_2 \end{pmatrix}^\top \begin{pmatrix} a & b \\ b & c \end{pmatrix} \begin{pmatrix} q_1 \\ q_2 \end{pmatrix} \right] \underline{G}_{(1)}(q'_1, q'_2, t; q_1, q_2, 0) \quad (6.1)$$

for each transverse dimension, with appropriate initial conditions set by either (i) appropriately normalized delta functions $\delta(q'_1 - q_1) \delta(q'_2 - q_2)$ or, perhaps more usefully, (ii) the functions the propagator is ultimately convolved with in the application [9, 10] (see below).

However, use of a numerical solution for the propagator will be complicated. For the large- N case, it was possible to use the known analytic form of a standard harmonic oscillator propagator to analytically perform most of the integrals in calculations of the overlap effects. Consider, for example, the overlap effects on the differential rate $d\Gamma/dx dy$ for $g \rightarrow ggg$ with

¹² The convention for labeling the four gluons in ref. [9] is slightly different than our convention here of fig. 5. The difference corresponds to relabeling $(\mathbf{b}_1, \mathbf{b}_2, \mathbf{b}_3, \mathbf{b}_4) \rightarrow (\mathbf{b}_3, \mathbf{b}_2, \mathbf{b}_4, \mathbf{b}_1)$ in the formula (5.11a) for the potential.

daughter energy fractions x , y , and $1-x-y$. The calculation of that rate involves integrals of the form, for example,¹³

$$\int_0^\infty d(\Delta t) \int_{\mathbf{B}', \mathbf{B}} \frac{B'_n}{(B')^2} \frac{B_m}{B^2} \exp\left(-\frac{1}{2}|M'|\Omega'(B')^2 - \frac{1}{2}|M|\Omega(B)^2\right) \times \nabla_{\mathbf{C}'_{34}}^{\bar{m}} \nabla_{\mathbf{C}'_{12}}^n G(\mathbf{C}'_{12}, \mathbf{C}'_{34}, \Delta t; \mathbf{C}_{12}, \mathbf{C}_{34}) \Big|_{\mathbf{C}'_{34}=0=\mathbf{C}_{12}; \mathbf{C}'_{12}=\mathbf{B}'; \mathbf{C}_{34}=\mathbf{B}}. \quad (6.2)$$

With a standard harmonic oscillator propagator, it was possible to do the two 2-dimensional integrals over \mathbf{B} and \mathbf{B}' analytically, leaving only the single Δt integral for numerical integration. With only a numerical result for the propagator, one must do the \mathbf{B} and \mathbf{B}' integrals numerically as well. Moreover, to make use of the rates to calculate the development of showers, one also needs x and y integrals involving $d\Gamma/dx dy$ (see ref. [14], for example). So, if the propagator is found numerically using (6.1), that numerical result would ultimately need to be used inside a numeric integration over $(\mathbf{B}, \mathbf{B}', \Delta t, x, y)$. That's not impossible but, we think, likely complicated to do accurately.

It would be *very* useful if there were, after all, some way to find an analytic solution to (6.1) for the propagator. Or alternatively, perhaps, to find some efficient expansion of the solution for which some integrals in (6.2), such as $(\mathbf{B}, \mathbf{B}')$, could be done analytically term by term.

Acknowledgments

My profound thanks to Han-Chih Chang. He participated in the early stages of this project and was the first of us to generate table I, using different [SU(3)-specific] methods than presented here, at a time (2015) when we were unaware of the then-contemporary work being carried out by Sjødahl and Thorén [20]. He demurred when recently offered co-authorship upon completion of this paper but is the reason this paper was written with the stylistic choice of using first-person plural.

I am also grateful to Howard Haber for discussions about SU(N) group theory, and to Diana Vaman and Dima Pesin for other useful conversations. This work was supported, in part, by the U.S. Department of Energy under Grant No. DE-SC0007984.

Appendix A: 6- j coefficients for four gluons in SU(N)

In this appendix, we give explicit constructions for the s -channel basis of 4-gluon singlet states, with primary focus on the five $(\sigma_1, \sigma_2, \sigma_3)=(+, +, +)$ singlets relevant to our application. Then we outline our calculation of the relevant 6- j coefficients.

¹³ The specific example (6.2) corresponds to fig. 6 and is taken from eq. (E7) of ref. [10], with various variables relabeled here, including the particle labels 1234 as described in footnote 12. For a slightly different but closely related example corresponding to fig. 5, see eq. (5.10) of ref. [9].

1. Projections that decompose $\text{Adj} \otimes \text{Adj}$

We start by discussing how to combine two gluons into a color representation R . The singlet state ($\mathbf{1}_s$) of two gluons is proportional to $\delta_{AB}|AB\rangle$. One way to make an adjoint state (Adj_a) is proportional to $f_{ABc}|AB\rangle$, where f_{abc} are the Lie algebra structure constants, given in terms of the fundamental-representation generators T_F^a as $f_{abc} = \frac{2}{i} \text{tr}([T_F^a, T_F^b]T_F^c)$. Here and throughout, we use the typical particle physics (as opposed to mathematics) normalization convention for the generators that $\text{tr}(T_F^a T_F^b) = \frac{1}{2} \delta^{ab}$. Another way to make an adjoint state (Adj_s) is $d_{ABC}|AB\rangle$, in terms of the completely symmetric $d_{abc} \equiv 2 \text{tr}(\{T_F^a, T_F^b\}T_F^c)$.

We'll find it convenient to write down the corresponding projection operators \mathcal{P}_R on the space $\text{Adj} \otimes \text{Adj}$, such that

$$|ab\rangle = (\mathcal{P}_1 + \mathcal{P}_{\text{Adj}_a} + \mathcal{P}_{\text{Adj}_s} + \mathcal{P}_{\mathbf{10}} + \mathcal{P}_{\overline{\mathbf{10}}} + \mathcal{P}_{\mathbf{27}} + \mathcal{P}_{\mathbf{0}})_{ab,AB}|AB\rangle. \quad (\text{A1})$$

The first three are

$$(\mathcal{P}_1)_{ab,AB} = \frac{1}{d_A} \delta_{ab} \delta_{AB}, \quad (\text{A2a})$$

$$(\mathcal{P}_{\text{Adj}_a})_{ab,AB} = \frac{1}{C_A} f_{abc} f_{ABc}, \quad (\text{A2b})$$

$$(\mathcal{P}_{\text{Adj}_s})_{ab,AB} = \frac{1}{\Delta} d_{abc} d_{ABc}, \quad (\text{A2c})$$

where d_A and C_A are the dimension and quadratic Casimir of the adjoint representation, and we've defined Δ by

$$d_{abc} d_{abd} = \Delta \delta_{cd}, \quad (\text{A3})$$

which is analogous to the relation

$$f_{abc} f_{abd} = C_A \delta_{cd}. \quad (\text{A4})$$

For $\text{SU}(N)$,

$$d_A = N^2 - 1, \quad C_A = N, \quad \Delta = \frac{N^2 - 4}{N}, \quad (\text{A5})$$

As appropriate to projection operators, (A2) is normalized so that each $(\mathcal{P}_R)^2 = \mathcal{P}_R$.

To find projection operators for the other states, split $\text{Adj} \otimes \text{Adj}$ into its symmetric and anti-symmetric combinations:

$$(\text{Adj} \otimes \text{Adj})_s = \mathbf{1} \oplus \text{Adj}_s \oplus \mathbf{27} \oplus \mathbf{0}, \quad (\text{A6})$$

$$(\text{Adj} \otimes \text{Adj})_a = \text{Adj}_a \oplus \mathbf{10} \oplus \overline{\mathbf{10}}. \quad (\text{A7})$$

We may then project $\mathbf{10} \oplus \overline{\mathbf{10}}$ by isolating the subspace of anti-symmetric color states and subtracting the part that belongs to Adj_a :

$$\begin{aligned} (\mathcal{P}_{\mathbf{10} \oplus \overline{\mathbf{10}}})_{ab,AB} &\equiv (\mathcal{P}_{\mathbf{10}} + \mathcal{P}_{\overline{\mathbf{10}}})_{ab,AB} = \frac{1}{2} (\delta_{aA} \delta_{bB} - \delta_{aB} \delta_{aA}) - (\mathcal{P}_{\text{Adj}_a})_{ab,AB} \\ &= \frac{1}{2} (\delta_{aA} \delta_{bB} - \delta_{aB} \delta_{aA}) - \frac{1}{C_A} f_{abc} f_{ABc}. \end{aligned} \quad (\text{A8})$$

We'll find later that we need not pick out $\mathbf{10}$ and $\overline{\mathbf{10}}$ separately, and so (A8) will be good enough.¹⁴

¹⁴ If desired, the $\mathbf{10}$ and $\overline{\mathbf{10}}$ could be separated using the methods of this appendix by following steps analogous to (A10–A12). If one finds an $\text{SU}(N)$ -covariant operator \mathcal{Z} that acts non-trivially on the subspace $\mathbf{10} \oplus \overline{\mathbf{10}}$ with the property that $\mathcal{Z}^2 = -1$ on that subspace, then $\frac{1}{2}(1 \mp i\mathcal{Z})\mathcal{P}_{\mathbf{10} \oplus \overline{\mathbf{10}}}$ gives two projection operators, dividing $\mathbf{10} \oplus \overline{\mathbf{10}}$ into the two conjugate complex representations. One can show that the operator $\mathcal{Z}_{ab,AB} \equiv \frac{1}{2}(f_{bAc} d_{aBc} + d_{bAc} f_{aBc})$ has the desired property.

Similarly, we can project “ $\mathbf{27} \oplus \mathbf{0}$ ” by isolating the subspace of symmetric states and then subtracting the pieces corresponding to the singlet and Adj_s:

$$\begin{aligned} (\mathcal{P}^{\mathbf{27} \oplus \mathbf{0}})_{ab,AB} &= \frac{1}{2}(\delta_{aA}\delta_{bB} + \delta_{aB}\delta_{aA}) - (\mathcal{P}_1)_{ab,AB} - (\mathcal{P}_{\text{Adj}_s})_{ab,AB} \\ &= \frac{1}{2}(\delta_{aA}\delta_{bB} + \delta_{aB}\delta_{aA}) - \frac{1}{d_A}\delta_{ab}\delta_{AB} - \frac{1}{\Delta}d_{abc}d_{ABc}. \end{aligned} \quad (\text{A9})$$

We need to isolate the two different representations “ $\mathbf{27}$ ” and “ $\mathbf{0}$ ”. If we find an $SU(N)$ -covariant operator Z that acts non-trivially on the subspace “ $\mathbf{27} \oplus \mathbf{0}$ ” with the property that $Z^2=1$ on that subspace, then $\frac{1}{2}(1 \mp Z)\mathcal{P}^{\mathbf{27} \oplus \mathbf{0}}$ would give two projection operators that split the subspace into “ $\mathbf{27}$ ” and “ $\mathbf{0}$ ”. One may verify that the operator

$$Z_{ab,AB} \equiv \frac{1}{2}(f_{aAc}f_{bBc} + f_{aBc}f_{bAc}) \quad (\text{A10})$$

has square

$$(Z^2)_{ab,AB} = Z_{ab,\alpha\beta}Z_{\alpha\beta,AB} = \frac{1}{2}(\delta_{aA}\delta_{bB} + \delta_{aB}\delta_{bA}) + \frac{N}{4}d_{abc}d_{ABc} + \delta_{ab}\delta_{AB} \quad (\text{A11})$$

for $SU(N)$, so that Z^2 acts as the identity on “ $\mathbf{27} \oplus \mathbf{0}$ ”. The resulting projection operators are

$$\begin{aligned} (\mathcal{P}^{\mathbf{27}})_{ab,AB} &= \frac{1}{4}(\delta_{aA}\delta_{bB} + \delta_{aB}\delta_{aA}) \mp \frac{1}{4}(f_{aAc}f_{bBc} + f_{aBc}f_{bAc}) \\ &\quad + (-\frac{1}{2} \pm \frac{N}{2})(\mathcal{P}_1)_{ab,AB} + (-\frac{1}{2} \pm \frac{N}{4})(\mathcal{P}_{\text{Adj}_s})_{ab,AB}, \end{aligned} \quad (\text{A12})$$

where the upper signs refer to “ $\mathbf{27}$ ” and the lower to “ $\mathbf{0}$ ”.

2. The 4-gluon color singlets

The $(\sigma_1, \sigma_2, \sigma_3)=(+, +, +)$ color singlets have a simple construction in terms of the projection operators: they are just

$$|s_{\mathcal{R}}\rangle \propto (\mathcal{P}_{\mathcal{R}})_{ABCD}|ABCD\rangle, \quad (\text{A13})$$

with the clarification that one should identify

$$|s_{\text{Adj}_{aa}}\rangle \propto (\mathcal{P}_{\text{Adj}_a})_{AB,CD}|ABCD\rangle, \quad (\text{A14})$$

$$|s_{\text{Adj}_{ss}}\rangle \propto (\mathcal{P}_{\text{Adj}_s})_{AB,CD}|ABCD\rangle, \quad (\text{A15})$$

$$|s^{\mathbf{10}+\overline{\mathbf{10}}}\rangle \equiv \frac{1}{\sqrt{2}}\left(|s^{\mathbf{10}}\rangle + |s^{\overline{\mathbf{10}}}\rangle\right) \propto (\mathcal{P}^{\mathbf{10} \oplus \overline{\mathbf{10}}})_{AB,CD}|ABCD\rangle. \quad (\text{A16})$$

The overlap matrix elements of table IV are then

$$\langle s_{\mathcal{R}}|t_{\mathcal{R}'}\rangle = \frac{(P_{\mathcal{R}})_{AB,CD}(P_{\mathcal{R}'})_{AC,BD}}{[(P_{\mathcal{R}})_{ab,cd}(P_{\mathcal{R}})_{ab,cd}]^{1/2}[(P_{\mathcal{R}'})_{\alpha\beta,\gamma\delta}(P_{\mathcal{R}'})_{\alpha\beta,\gamma\delta}]^{1/2}}, \quad (\text{A17})$$

where the denominator accounts for normalization of the 4-gluon states (A13). They may be computed using the following $SU(N)$ formulas for the contraction of four or fewer f_{abc} 's and d_{abc} 's.

3. Useful $SU(N)$ relations

Useful $SU(N)$ relations for the preceding calculations include [25]

$$\text{tr}(D^a) = 0, \tag{A18}$$

$$\text{tr}(F^a F^b F^c F^d) = \delta_{ab}\delta_{cd} + \delta_{ad}\delta_{bc} + \frac{N}{4}(d_{abe}d_{cde} - d_{ace}d_{bde} + d_{ade}d_{bce}), \tag{A19}$$

$$\text{tr}(F^a F^b D^c D^d) = \frac{(N^2-4)}{N^2}(\delta_{ab}\delta_{cd} - \delta_{ac}\delta_{bd}) + \frac{(N^2-8)}{4N}(d_{abe}d_{cde} - d_{ace}d_{bde}) + \frac{N}{4}d_{ade}d_{bce}, \tag{A20}$$

$$\text{tr}(F^a D^b F^c D^d) = \frac{N}{4}(d_{abe}d_{cde} - d_{ace}d_{bde} + d_{ade}d_{bce}), \tag{A21}$$

$$\text{tr}(D^a D^b D^c D^d) = \frac{(N^2-4)}{N^2}(\delta_{ab}\delta_{cd} + \delta_{ad}\delta_{bc}) + \frac{(N^2-16)}{4N}(d_{abe}d_{cde} + d_{ade}d_{bce}) - \frac{N}{4}d_{ace}d_{bde}, \tag{A22}$$

$$[D^a, D^b]_{cd} = if_{abe}(F^e)_{cd} - \frac{2}{N}(\delta_{ac}\delta_{bd} - \delta_{ad}\delta_{bc}), \tag{A23}$$

where

$$(F^a)_{bc} \equiv -if_{abc}, \quad (D^a)_{bc} \equiv d_{abc}. \tag{A24}$$

Ref. [26] gives a very useful summary of these and many other relations, drawn from (and correcting a few typographic errors in) refs. [21, 25, 27–30].

- [1] L. D. Landau and I. Pomeranchuk, “Limits of applicability of the theory of bremsstrahlung electrons and pair production at high-energies,” *Dokl. Akad. Nauk Ser. Fiz.* **92** (1953) 535; “Electron cascade process at very high energies,” *ibid.* 735. These two papers are also available in English in L. Landau, *The Collected Papers of L.D. Landau* (Pergamon Press, New York, 1965).
- [2] A. B. Migdal, “Bremsstrahlung and pair production in condensed media at high-energies,” *Phys. Rev.* **103**, 1811 (1956);
- [3] R. Baier, Y. L. Dokshitzer, A. H. Mueller, S. Peigne and D. Schiff, “The Landau-Pomeranchuk-Migdal effect in QED,” *Nucl. Phys. B* **478**, 577 (1996) [arXiv:hep-ph/9604327]; “Radiative energy loss of high-energy quarks and gluons in a finite volume quark - gluon plasma,” *ibid.* **483**, 291 (1997) [arXiv:hep-ph/9607355].
- [4] R. Baier, Y. L. Dokshitzer, A. H. Mueller, S. Peigne and D. Schiff, “Radiative energy loss and p_{\perp} -broadening of high energy partons in nuclei,” *ibid.* **484** (1997) [arXiv:hep-ph/9608322].
- [5] B. G. Zakharov, “Fully quantum treatment of the Landau-Pomeranchuk-Migdal effect in QED and QCD,” *JETP Lett.* **63**, 952 (1996) [arXiv:hep-ph/9607440]; “Radiative energy loss of high-energy quarks in finite size nuclear matter an quark - gluon plasma,” *ibid.* **65**, 615 (1997) [*Pisma Zh. Eksp. Teor. Fiz.* **63**, 952 (1996)] [arXiv:hep-ph/9607440].
- [6] J. P. Blaizot and Y. Mehtar-Tani, “Renormalization of the jet-quenching parameter,” *Nucl. Phys. A* **929**, 202 (2014) [arXiv:1403.2323 [hep-ph]].
- [7] E. Iancu, “The non-linear evolution of jet quenching,” *JHEP* **1410**, 95 (2014) [arXiv:1403.1996 [hep-ph]].
- [8] B. Wu, “Radiative energy loss and radiative p_{\perp} -broadening of high-energy partons in QCD matter,” *JHEP* **1412**, 081 (2014) [arXiv:1408.5459 [hep-ph]].
- [9] P. Arnold and S. Iqbal, “The LPM effect in sequential bremsstrahlung,” *JHEP* **04**, 070 (2015) [*erratum JHEP* **09**, 072 (2016)] [arXiv:1501.04964 [hep-ph]].
- [10] P. Arnold, H. C. Chang and S. Iqbal, “The LPM effect in sequential bremsstrahlung 2: factorization,” *JHEP* **1609**, 078 (2016) [arXiv:1605.07624 [hep-ph]];

- [11] P. Arnold, H. C. Chang and S. Iqbal, “The LPM effect in sequential bremsstrahlung: dimensional regularization,” JHEP **1610**, 100 (2016) [arXiv:1606.08853 [hep-ph]].
- [12] P. Arnold, H. C. Chang and S. Iqbal, “The LPM effect in sequential bremsstrahlung: 4-gluon vertices,” JHEP **1610**, 124 (2016) [arXiv:1608.05718 [hep-ph]].
- [13] P. Arnold and S. Iqbal, “In-medium loop corrections and longitudinally polarized gauge bosons in high-energy showers,” JHEP **1812**, 120 (2018) [arXiv:1806.08796 [hep-ph]].
- [14] P. Arnold, S. Iqbal and T. Rase, “Strong- vs. weak-coupling pictures of jet quenching: a dry run using QED,” arXiv:1810.06578 [hep-ph].
- [15] A. R. Edmonds, Angular Momentum in Quantum Mechanics, 2nd edition (Princeton University Press, 1960).
- [16] P. Arnold, “Multi-particle potentials from light-like Wilson lines in quark-gluon plasmas: a generalized relation of in-medium splitting rates to jet-quenching parameters \hat{q} ,” Phys. Rev. D **99**, no. 5, 054017 (2019) [arXiv:1901.05475 [hep-ph]].
- [17] H. Liu, K. Rajagopal and U. A. Wiedemann, “Calculating the jet quenching parameter from AdS/CFT,” Phys. Rev. Lett. **97**, 182301 (2006) [hep-ph/0605178].
- [18] H. Liu, K. Rajagopal and U. A. Wiedemann, “Wilson loops in heavy ion collisions and their calculation in AdS/CFT,” JHEP **0703**, 066 (2007) [hep-ph/0612168];
- [19] S. Caron-Huot, “O(g) plasma effects in jet quenching,” Phys. Rev. D **79**, 065039 (2009) [arXiv:0811.1603 [hep-ph]].
- [20] M. Sjodahl and J. Thorén, “Decomposing color structure into multiplet bases,” JHEP **1509**, 055 (2015) [arXiv:1507.03814 [hep-ph]].
- [21] L. M. Kaplan and M. Resnikoff, “Matrix Products and the Explicit 3, 6, 9, and 12- j Coefficients of the Regular Representation of $SU(n)$,” J. Math. Phys. **8**, 2194 (1967).
- [22] R. P. Bickerstaff, P. H. Butler, M. B. Butts, R. W. Haase and M. F. Reid, “ $3jm$ and $6j$ tables for some bases of SU_6 and SU_3 ,” J. Phys. A **15**, 1087 (1982).
- [23] H. Elvang, P. Cvitanić and A. D. Kennedy, “Diagrammatic Young projection operators for $U(n)$,” hep-th/0307186.
- [24] P. Cvitanić, *Group theory: Birdtracks, Lie’s, and Exceptional Groups* (Princeton University Press, 2008), also available at <http://birdtracks.eu/version9.0/GroupTheory.pdf>.
- [25] J. A. de Azcarraga, A. J. Macfarlane, A. J. Mountain and J. C. Pérez Bueno, “Invariant tensors for simple groups,” Nucl. Phys. B **510**, 657 (1998) [physics/9706006].
- [26] H. Haber, “Useful relations among the generators in the defining and adjoint representations of $SU(N)$ ” (unpublished), <http://scipp.ucsc.edu/~haber/webpage/sunid.pdf>.
- [27] A. J. MacFarlane, A. Sudbery and P. H. Weisz, “On Gell-Mann’s lambda-matrices, d- and f-tensors, octets, and parametrizations of $SU(3)$,” Commun. Math. Phys. **11**, 77 (1968).
- [28] V. S. Fadin and R. Fiore, “Non-forward NLO BFKL kernel,” Phys. Rev. D **72**, 014018 (2005) [hep-ph/0502045].
- [29] R. Cutler and D. W. Sivers, “Quantum-chromodynamic gluon contributions to large- p_T reactions,” Phys. Rev. D **17**, 196 (1978).
- [30] P. Tarjanne, “A group theoretical model for strong interaction dynamics,” Annales Academiae Scientiarum Fennicae Ser. A, VI. Physica **105**, 3 (1962).